






Spectral phase singularity and topological behavior in perfect absorptionMengqi Liu ^{1,2} Weijin Chen,² Guangwei Hu ³ Shanhui Fan ³ Demetrios N. Christodoulides,⁴
Changying Zhao ^{1,*} and Cheng-Wei Qiu ^{2,†}¹*Institute of Engineering Thermophysics, MOE Key Laboratory for Power Machinery and Engineering, School of Mechanical Engineering, Shanghai Jiao Tong University, Shanghai 200240, China*²*Department of Electrical and Computer Engineering, National University of Singapore, Singapore 117583, Singapore*³*Department of Electrical Engineering, Ginzton Laboratory, Stanford University, Stanford, California 94305, USA*⁴*Center for Research and Education in Optics and Lasers (CREOL), The College of Optics and Photonics, University of Central Florida, Orlando, Florida 32816, USA* (Received 13 September 2022; revised 25 April 2023; accepted 26 April 2023; published 8 June 2023)

Perfect absorbers, which can achieve total absorption of all incoming energy, have been extensively studied in the last decades for various important technologies in general wave systems. Here, we show that perfect absorption (PA) is generically associated with topological spectral phase singularity (SPS), carrying conserved and tunable quantized topological invariants in spectral space. The order of topological invariant $\tilde{\nu}$ depends on the number of degenerate outgoing channels. Two commonly studied absorbers, mirror-backed and all-dielectric structures, are reexamined from a topological perspective to reveal the generation, evolution, and annihilation of SPSs with $\tilde{\nu} = \pm 1$ or even high orders (i.e., $\tilde{\nu} = \pm 2, \pm 4$). A strategy based on charge conservation of SPSs to design dual-band perfect absorbers has been established. Our findings establish the topological origin of the robust existence of PA. More broadly, in this letter, we highlight topology as the fundamental property of conventional scattering behaviors. This insight could lead to opportunities in applications such as biosensing, topological metasurfaces, and micro/nano thermal radiation.

DOI: [10.1103/PhysRevB.107.L241403](https://doi.org/10.1103/PhysRevB.107.L241403)

Absorption of light represents one of the most fundamental aspects of light-matter interactions. Over the last decades, many efforts have been dedicated to designing perfect absorbers [1] in nearly every part of the whole electromagnetic spectrum [2–6], motivated by applications in high-precision sensing [7], photovoltaic/photothermal devices [8–10], superresolution imaging [11,12], cloaking [13], and so on. Recently, benefiting from the great development of advanced nanofabrication technologies and in-depth research of photonic theories, various kinds of configurations have been proposed, including Dallenbach and Sailsbury absorbers [14], photonic crystals [15], multilayers [16], metal-insulator-metal (MIM) or hyperbolic metamaterials [17,18], all-dielectric metasurfaces [19], and even coherent perfect absorbers [20,21]. However, despite extensive studies in theories, structure design, multifunctional properties, or even active devices, the underlying topological behavior of perfect absorption (PA) has seldom been discussed.

Theoretically, PA ensures that all the incoming energy can be thoroughly absorbed without any scattering event. For extensively studied mirror-backed perfect absorbers, for example, the PA can be generally achieved when the only reflection channel is completely suppressed. Before, such zero-reflection points were reportedly associated with a phase jump in the one-dimensional (1D) reflection phase graph

[22–25] but locking up exciting topological phenomena. More recently, by extending the view of reflection phase spectra into two-dimensional (2D) spectral-parameter spaces, a phase vortex described by nonzero topological charges, namely, spectral phase singularities (SPSs) here, could be observed [14,26–30], which were then verified in different systems composed of metal arrays [14], atomically thin 2D materials [28], or epsilon-near-zero materials [31]. Our previous work focused on the evolution of reflection phase singularity pairs (zero reflection) in one-port systems [31], where PA could always be observed at this singular phase. However, it should be noted that all the above findings, including PA points and SPSs, are occasionally found by random parameter sweep for some specific configurations. Then one open question may arise: Can all PA in general be topological? It thereby inspires us to rethink the underlying physics between PA and topology in a more general view to provide a universal design principle for PA via involving SPSs. An intuitive understanding of why such SPSs exist and are robust was previously lacking, and there is no general physical description of such PA-related SPSs. Additionally, although a +2 SPS has been reported in the synthetic phase [28], i.e., $\arg(r_p/r_s)$ (r_p, r_s being reflection coefficients under p or s polarization), the explicit generation rule of higher-order SPSs and their connections between perfect absorbers have never been revealed.

In this letter, we first reinterpret PA from a topological perspective based on temporal coupled-mode theory (TCMT) [32,33]. The generic principles to identify the order of SPSs at PA points are explicitly established, providing a universal

*changying.zhao@sjtu.edu.cn

†chengwei.qiu@nus.edu.sg

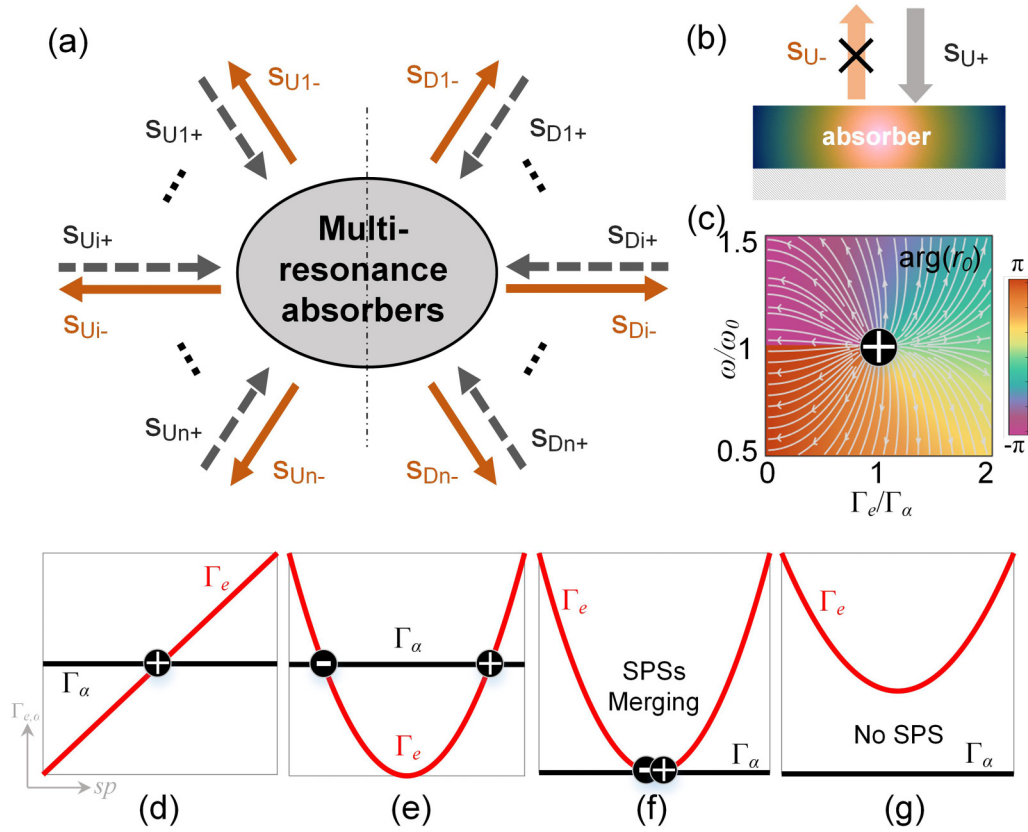


FIG. 1. Topological nature of perfect absorption (PA) points associated with spectral phase singularities (SPSs). (a) Schematic of the multiport multimode system. The subscripts U and D denote the upper and downside channels. (b) The mirror-backed one-port system, along with (c) its typical reflection phase in parameter space. (d)–(g) Possible relations between radiative loss Γ_e and material loss Γ_α at $\omega = \omega_0$; linear type for all Γ_α ; linear type for Γ_e in (d) and hyperbolic type for Γ_e in (e)–(g). The sp could represent the system parameter, like thickness, period, or incident angle.

guideline of designing perfect absorbers in different systems. The generation, evolution, and annihilation of SPSs with different orders have been analyzed in widely studied absorbers. Further, the revealed topological behaviors of PA-associated SPSs also stimulate us to establish a method to design dual-band perfect absorbers. The topological robustness of PA in other parameter spaces and the possibility of achieving other orders of SPSs are also discussed.

To build a general view, we begin with a multiport system ($N = 2n$ channels) in Fig. 1(a), which has mirror symmetry and supports m resonant modes. Based on TCMT, one can obtain the scattering matrix [34]:

$$\mathbf{S} = \mathbf{C} \left[\mathbf{I} - \frac{\mathbf{D}^* \mathbf{D}^T}{i(\omega - \boldsymbol{\Omega}) + \boldsymbol{\Gamma}_e + \boldsymbol{\Gamma}_\alpha} \right] = \begin{bmatrix} \mathbf{S}_{(U,U)} & \mathbf{S}_{(U,D)} \\ \mathbf{S}_{(D,U)} & \mathbf{S}_{(D,D)} \end{bmatrix}, \quad (1)$$

where \mathbf{C} is a $N \times N$ matrix describing the scattering process without resonances, \mathbf{D} denotes the coupling matrix between resonances (frequency $\boldsymbol{\Omega} = [\omega_1, \omega_2, \dots, \omega_l, \dots, \omega_m]^T$) and outgoing channels. The $\boldsymbol{\Gamma}_e = [\Gamma_e^1, \Gamma_e^2, \dots, \Gamma_e^l, \dots, \Gamma_e^m]^T$ and $\boldsymbol{\Gamma}_\alpha = [\Gamma_\alpha^1, \Gamma_\alpha^2, \dots, \Gamma_\alpha^l, \dots, \Gamma_\alpha^m]^T$ present the radiative and non-radiative (material) losses of the systems, respectively. The U_X, D_Y mark the X th upper and Y th down channels. Being constrained by reciprocity, there are $S_{(U_X, D_Y)} = S_{(D_Y, U_X)}$ and $S_{(U_X, U_Y)} = S_{(D_X, D_Y)}$ ($X, Y \in [1, n]$). Here, we merely con-

sider incident light from the upper plane. Then the scattering matrix reduces to $\mathbf{S} = [\mathbf{S}_{(U,U)}, \mathbf{S}_{(U,D)}]$, where the element $S_{(U_X, U_Y)}$ [$S_{(U_X, D_Y)}$] reads reflection (transmission) coefficients account for light transporting from U_X to U_Y (D_Y). Then absorption can be calculated by energy conservation: $A = 1 - \sum_{X=1}^n \sum_{Y=1}^n [|S_{(U_X, U_Y)}|^2 + |S_{(U_X, D_Y)}|^2]$, so that every matrix element of \mathbf{S} being zero is both necessary and sufficient to create PA ($A = 1$). The degenerate zeros are associated with ill-defined points in the transmission phase $\varphi_{l, X, Y} = \arg[S_{(U_X, D_Y)}]$ and reflection phase $\varphi_{r, X, Y} = \arg[S_{(U_X, U_Y)}]$. PA thus in general corresponds to a set of degenerate SPSs.

We suppose that resonant modes are orthogonal unless otherwise stated. Then one can obtain elements in Eq. (1) expressed by

$$S_{(U_X, D_Y)} = \delta_{X,Y} \tilde{r}_X - \sum_{l=1}^m \frac{\beta_l \cdot \tilde{r}_X \gamma_e^l + \tilde{t}_X \gamma_e^l}{i(\omega - \omega_l) + \Gamma_e^l + \Gamma_\alpha^l}, \quad (2a)$$

$$S_{(U_X, U_Y)} = \delta_{X,Y} \tilde{r}_X - \sum_{l=1}^m \frac{\tilde{r}_X \gamma_e^l + \beta_l \cdot \tilde{t}_X \gamma_e^l}{i(\omega - \omega_l) + \Gamma_e^l + \Gamma_\alpha^l}, \quad (2b)$$

where \tilde{r}_X and \tilde{t}_X are the direct reflection and transmission coefficients in \mathbf{C} . We assume that the coupling efficiency between the l th mode and different channels are the same; hence, $\gamma_e^l = 2\Gamma_e^l/N$. The mode parity is encoded in $\beta_l = \pm 1$ (+1 for symmetric modes, -1 for asymmetric modes). Here, $\delta_{X,Y}$ is the Dirac function. The details of derivation can be

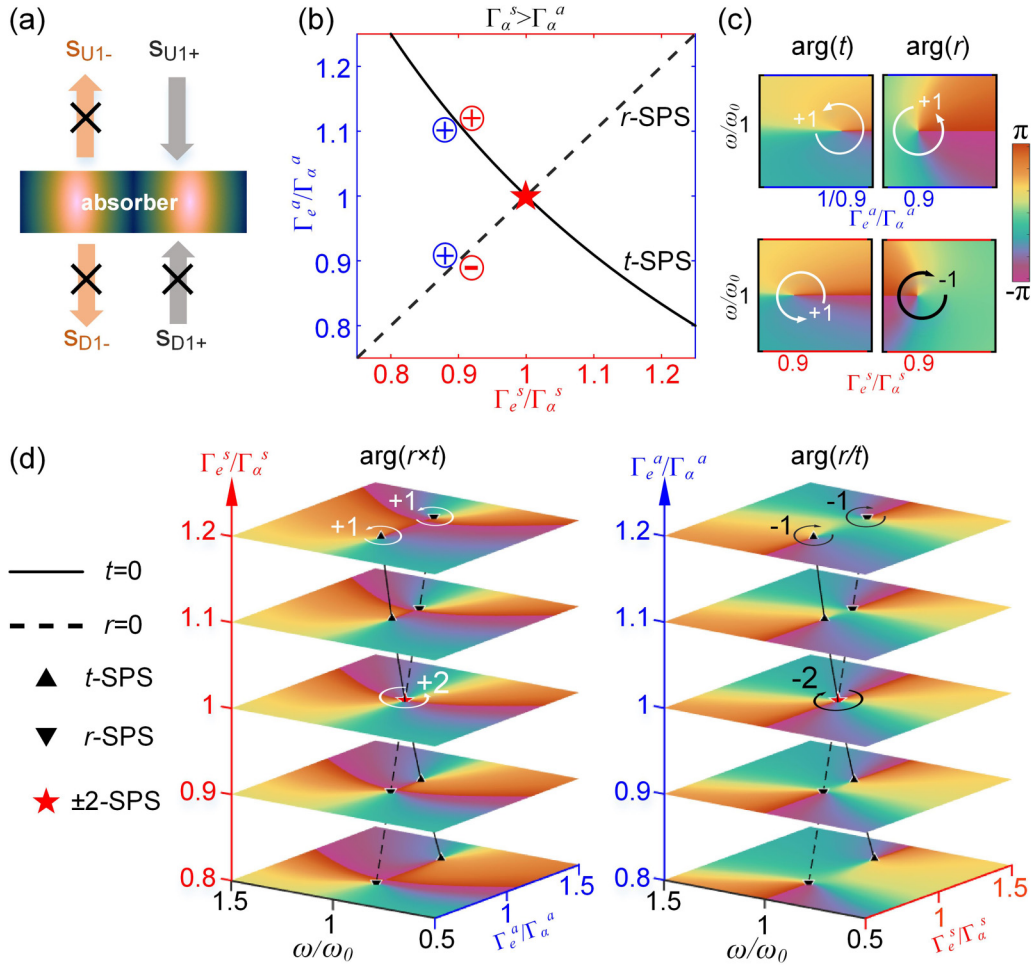


FIG. 2. High-order perfect absorption (PA)-related spectral phase singularities (SPSs). (a) Schematic of the two-port system. (b) Evolution trajectory of reflection-type SPSs ($r = 0$, dashed line) and transmission-type SPSs ($t = 0$, full line). The red pentagram denotes the position of PA point. The topological charges are marked in different projection planes: $\omega - \Gamma_e^a/\Gamma_\alpha^a$ space (blue) and $\omega - \Gamma_e^s/\Gamma_\alpha^s$ space (red), along with (c) the corresponding reflection or transmission phase. (d) Generation rules of high-order SPSs viewing the phase of $\varphi_{rxt} = \arg(r \times t)$ in $\omega - \Gamma_e^a/\Gamma_\alpha^a$ space (left) and $\varphi_{r/t} = \arg(r/t)$ in $\omega - \Gamma_e^s/\Gamma_\alpha^s$ space (right).

found in the Supplemental Material [34]. In the following, two basic perfect absorbers with different ports are considered to reveal the underlying topological behaviors.

Some of the most commonly studied perfect absorbers are mirror-backed structures with no diffraction in Fig. 1(b). The upper structure could be shaped using metamaterials or metasurfaces [3,42,43]. In this system ($N = 1$), PA could be achieved if and only if there is only one resonant mode ($m = 1, \omega_0$) [44]. Then Eqs. (2a) and (2b) are simplified to $r_0 = S_{(U_1, U_1)} = \frac{-i(\omega - \omega_0) + \Gamma_e - \Gamma_\alpha}{i(\omega - \omega_0) + \Gamma_e + \Gamma_\alpha}$, $t_0 \equiv 0$. The reflection phase in $\omega - \Gamma_e/\Gamma_\alpha$ space is given in Fig. 1(c). There is a phase vortex located exactly at $\omega = \omega_0, \Gamma_e = \Gamma_\alpha$ known as a critical coupling condition [45] predicting the presence of PA. Although this condition was proposed many years ago, the phase evolution and topological properties around this critical point in spectral space have seldom been discussed. By tracing an anticlockwise closed loop around the singularity, a total accumulated phase of $+2\pi$ can be obtained, implying an integer winding number $v = +1$ calculated by

$$v = \frac{1}{2\pi} \oint d\varphi, \quad v \in \mathbb{Z}, \quad (3)$$

with φ being the reflection phase $\varphi_0 = \arg(r_0)$ in this case. Similar definitions of topological invariants can also be found in describing bound states in the continuum (BICs) in momentum space [46–48], topological defects of 2D spins [49], spatial vortex beams [50,51], etc. Such findings reveal that the topological nature is also inherently prevalent for PA at critical coupling since the annihilation of PA-related SPSs is only possible when topological charges of an opposite sign are present. Some works have already studied ± 1 phase singularities for specific cases [14,52], where the topological charges are created in, i.e., frequency-period or frequency-incident angles that influence the competitive values of $\Gamma_{e,\alpha}$. Figure 1(d) shows a similar situation in Fig. 1(c), where a $+1$ SPS arises when the system changes from overdamped ($\Gamma_\alpha > \Gamma_e$)

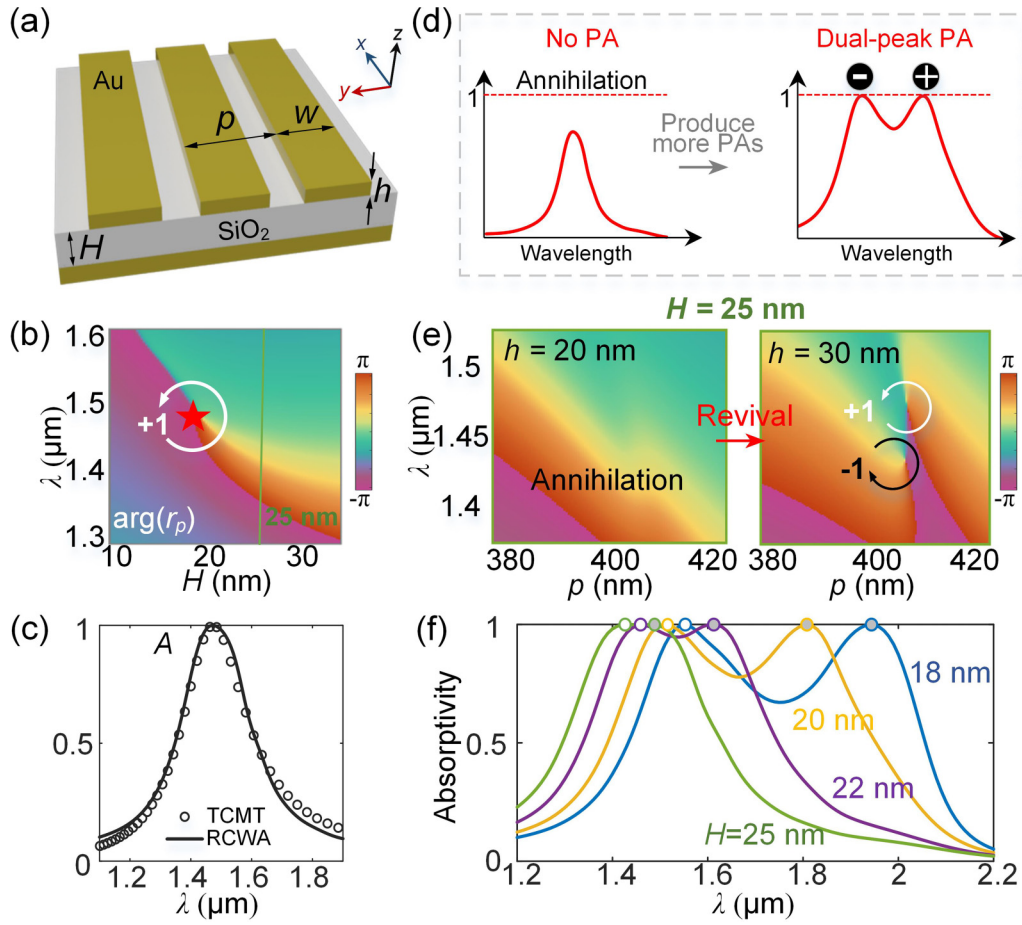


FIG. 3. Topological behaviors of spectral phase singularities (SPSs) in metal-insulator-metal (MIM) perfect absorbers. (a) Schematic of the MIM absorber, composed of a bottom Au mirror, SiO₂ interlayer, and Au gratings. The p polarization (E_x , H_y , k_z) is considered. (b) Reflection phase (φ_r) viewing in λ - H space. The +1 SPS is denoted with a red star, along with (c) the corresponding perfect absorption (PA) spectrum ($H = 18$ nm). (d) A design principle for dual-band perfect absorbers based on the charge evolution of topological phase singularity: (left) no PA with annihilated SPSs and (right) dual-peak PA points with two revival SPSs. (e) Typical cases for presenting the evolution of SPSs in λ - p space, at $H = 25$ nm and different h . (f) Absorption spectra with dual PA peaks for cases with different H were obtained based on the method in (d). The circles in white or gray represent PA points associated with -1 or $+1$ SPSs in λ - p space.

to underdamped ($\Gamma_\alpha < \Gamma_e$). As the profile of Γ_e becomes parabolic in Fig. 1(e), there is another -1 SPS (underdamped \rightarrow overdamped). By moving Γ_α down, two opposite SPSs will move synchronously and merge at the critical position in Fig. 1(f). In analogy with merging BICs [53], the magnitude of absorptivity still tends to $A \rightarrow 1$ if $\Gamma_\alpha \neq 0$. Particularly, the case of $\Gamma_\alpha = 0$ corresponds to the appearance of BIC in photonic systems. Afterward, the annihilation of two SPSs happens with no PA when Γ_α further moves down [Fig. 1(g)].

When more channels are involved in the scattering process, the condition of PA corresponds to a set of degenerate SPSs, and the associated topological invariant \tilde{v} shows as

$$\tilde{v} = \sum_{X,Y=1}^n [p_{X,Y} \cdot v_{(U_X, U_Y)} + q_{X,Y} \cdot v_{(U_X, D_Y)}] = N \cdot v_{(U_1, U_1)}, \quad (4)$$

where $p_{X,Y} = v_{(U_1, U_1)}/v_{(U_X, U_Y)}$ and $q_{X,Y} = v_{(U_1, U_1)}/v_{(U_X, D_Y)}$ are the signs of SPSs obtained for different channels in the same spectral space. The high-order SPS with \tilde{v} can be observed by checking the phase of $\varphi = \arg\{\prod_{X,Y=1}^n [S_{(U_X, U_Y)}]^{p_{X,Y}} [S_{(U_X, D_Y)}]^{q_{X,Y}}\}$ with $p_{X,Y}, q_{X,Y} = \pm 1$.

For example, as for a two-port absorber ($N = 2$) in Fig. 2(a), there are two resonant modes: asymmetric (label a) and symmetric (label s) modes. Thus, Eqs. (2a) and (2b) reduce to $t = S_{(U_1, D_1)} = 1 - \frac{\Gamma_e^a}{i(\omega - \omega_a) + \Gamma_e^a + \Gamma_\alpha^a} - \frac{\Gamma_e^s}{i(\omega - \omega_s) + \Gamma_e^s + \Gamma_\alpha^s}$ and $r = S_{(U_1, U_1)} = \frac{\Gamma_e^a}{i(\omega - \omega_a) + \Gamma_e^a + \Gamma_\alpha^a} - \frac{\Gamma_e^s}{i(\omega - \omega_s) + \Gamma_e^s + \Gamma_\alpha^s}$. At the on-resonance condition $\omega = \omega_a = \omega_s$, the requirement of $t, r = 0$ leads to

$$\Gamma_e^s \Gamma_e^a = \Gamma_\alpha^s \Gamma_\alpha^a, \quad (5a)$$

$$\frac{\Gamma_e^s}{\Gamma_e^a} = \frac{\Gamma_\alpha^s}{\Gamma_\alpha^a}. \quad (5b)$$

In Fig. 2(b), PA (red star) is generated at the intersection between the nodal lines of t -SPS and r -SPS, where the degenerate critical coupling condition [54] is satisfied ($\Gamma_\alpha^a = \Gamma_e^a, \Gamma_\alpha^s = \Gamma_e^s$). Assuming $\Gamma_\alpha^s > \Gamma_\alpha^a$, one can observe +1 t -SPSs located in both $\omega - \Gamma_e^a/\Gamma_\alpha^a$ and $\omega - \Gamma_e^s/\Gamma_\alpha^s$ spaces [Fig. 2(c), left], while the reflection singularity has a topological charge of +1 in $\omega - \Gamma_e^a/\Gamma_\alpha^a$ space but -1 in $\omega - \Gamma_e^s/\Gamma_\alpha^s$ space [Fig. 2(c), right]. PA occurs when two nodal lines intersect, creating a degenerate singularity. Using Eq. (4),

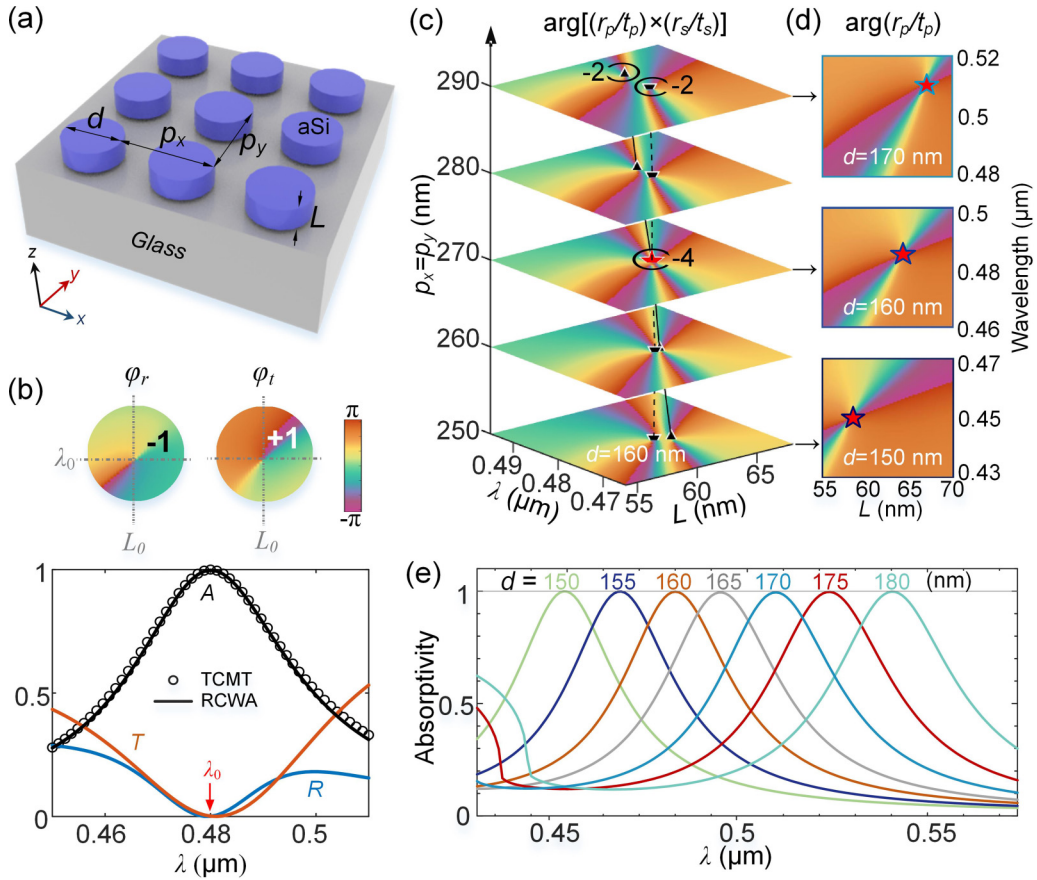


FIG. 4. Topological behaviors of high-order spectral phase singularities (SPSs) in all-dielectric perfect absorbers. (a) Schematic of the all-dielectric absorber, composed of periodic a-Si nanodisks sitting on a glass substrate. (b) Absorption (black), reflection (blue), and transmission (red) spectra, together with the phase φ_r ($v = -1$) and φ_t ($v = +1$) in λ - L space. The λ_0 denotes the wavelength of PA point. (c) Generation of high-order SPSs in the phase of $\arg[(r_p/t_p) \times (r_s/t_s)]$ changing with different p_x at a fixed $d = 160$ nm. (d) Three typical phases of $\arg(r_p/t_p)$: (top) $p_x = 290$ nm, $d = 170$ nm; (middle) $p_x = 270$ nm, $d = 160$ nm; and (bottom) $p_x = 250$ nm, $d = 150$ nm. (e) Topological robustness of high-order SPSs: absorption spectra with PA peaks as the diameter d changes.

one can obtain $\tilde{v} = v_r + v_t = +1 + (+1) = +2$ in ω - $\Gamma_e^a/\Gamma_\alpha^a$ space ($p_r, q_t = +1$) and $\tilde{v} = v_r - v_t = -1 - (+1) = -2$ in ω - $\Gamma_e^s/\Gamma_\alpha^s$ space ($p_r = +1, q_t = -1$), considering the phase of $\varphi_{r \times t} = \arg(r \times t)$ [Fig. 2(d), left] and $\varphi_{r/t} = \arg(r/t)$ [Fig. 2(d), right], respectively. In other words, in a two-port system, the appearance of PA corresponds to the generation of ± 2 -order SPSs. When more channels are involved, the appearance of PA should be associated with high-order degenerate SPSs.

Next, we will give examples to demonstrate the underlying topological behaviors of PA, which empowers opportunities to design perfect absorbers with more diversity. Figure 3(a) shows a MIM structure with 1D Au gratings (period p , width w , and thickness h) adopted from Ref. [55]. The absorption enhancement can be realized by properly exciting magnetic polaritons within the dielectric interlayer (height H). For a given Au grating ($p = 400$ nm, $w = 250$ nm, and $h = 20$ nm), by sweeping the reflection phase in λ - H space under p -polarization, a $+1$ SPS in Fig. 3(b) with PA spectrum in Fig. 3(c) can be obtained. Such an individual SPS (or PA) will be topologically robust unless large parameter changes are introduced into the system (Fig. S6 in the Supplemental Material [34]), which has not been uncovered before. Based

on the charge conservation of SPSs, here, we can propose a direct and simple method to achieve dual-band PA. The existing dual- or multiband absorbers mainly rely on either combining two or more resonators with different geometric sizes to form a super unit [36–39,56] or stack multilayer [40,57] with separated resonant frequencies. Such designs are more demanding for nanofabrication technologies, and it may be difficult to ensure unity absorptivity for all peaks simultaneously. Instead, the intrinsically topological nature of PA will provide a platform to overcome these challenges, as sketched in Fig. 3(d). Considering a non-PA spectrum that may be ascribed to the annihilation of two SPSs [Fig. 1(g)], it in turn provides an opportunity to revive these singularities by tuning the balance between radiative and nonradiative losses of the whole system. For instance, at $H = 25$ nm, there are no visible SPSs in λ - p space [Fig. 3(e), left] because the structures do not satisfy the critical coupling condition. By increasing the thickness of the Au grating (reducing the magnitude of radiative loss), two SPSs with opposite topological invariants emerge [Fig. 3(e), right], thus enabling dual-band PA in Fig. 3(f) (green line). As such, for different H far away from the red star in Fig. 3(b), one can always obtain dual-peak PA spectra using the above approach. In these cases, PA can

be ensured all the time, and the spectral distance between two PA peaks can be flexibly tailored by shaping the positions of two SPSs. The intrinsic topological nature of PA-related SPSs governs the evolution of absorption spectra. The proposed method is also applicable to other systems with distinct advantages like maintaining robust PA performance, releasing complex structure requirements, and providing universal design principles (Note 3 in the Supplemental Material [34]).

In Fig. 4, we show the topological behavior of SPSs for an all-dielectric absorber which consists of periodic a-Si ($\epsilon_{\text{aSi}} = 3.43 + i0.09$) nanodisks sitting on a glass ($\epsilon_g = 1.46$) substrate. The coexistence and destructive interference of electric (approximately symmetric) and magnetic (approximately asymmetric) resonances ensures the complete cancellation of both reflection and transmission. The period $p_x = p_y$, height L , and diameter d contribute to shaping the competitive balance between material and radiative losses of two modes. Figure 4(b) shows the absorption (black), reflection (blue), and transmission (red) spectra under an optimal condition ($p_x = 270$ nm, $L_0 = 62$ nm, and $d = 160$ nm), associated with a -1 r -SPS and a $+1$ t -SPS at $\lambda_0 = 0.48$ μm and L_0 [Fig. 4(b), top], respectively. Since the whole system is in-plane symmetric, PA also becomes polarization insensitive, ensuring the appearance of -4 SPS ($N = 4$ considering p and s waves) by viewing the phase of $\arg[(r_p/t_p) \times (r_s/t_s)]$ in Fig. 4(c). The appearance of two separated -2 SPSs is ascribed to the degeneracy of reflection (left, $v_{r_p} + v_{r_s}$) or transmission (right, $-v_{t_p} - v_{t_s}$) channels under two polarization states. Consistently, as for an individual polarization, a clear -2 SPS ($\tilde{v} = v_{r_p} - v_{t_p}$) could be obtained [Fig. 4(d), middle]. Owing to the topological robustness of PA-related SPSs, this -2 SPS will always exist, even though the geometric parameters are moderately changed. For example, as for the nonideal cases of $p_x = 290$ nm and $p_x = 250$ nm in Fig. 4(c), the -2 SPSs can also be ensured by increasing [Fig. 4(d), top] or decreasing [Fig. 4(d), bottom] the value of d . Figure 4(e) shows the continuous evolution of the selected PA spectra as the diameter of the nanodisk changes, where PA can always be realized. In contrast, most reported all-dielectric absorbers can only work at a specific wavelength [54,58–61]. Even though another PA may also be found by sparing no effort to sweep the geometric parameters, the underlying topological behavior behind the continuous evolution of PA has not been fully understood.

The above PA properties are discussed under normal incidence, but several works have also paid attention to off- 0° performance. In analogy with accidental BICs [53,62–64], the existence of off- 0° PA does not require finetuning of system parameters. The small changes in parameters simply shift the position of these PA points, which are ascribed to the topological robustness of SPSs. In Note 4 in the Supplemental Material [34], we consider a one-port structure composed of upper polar material and dielectric interlayer in Fig. S9 in the Supplemental Material [34]. Around the epsilon-near-pole (ENP) wavelength, one can expect several SPSs in the reflection phase under two polarizations, owing to the interference effects between Fabry-Perot resonances and ENP modes.

For both ± 1 and ± 2 (polarization-insensitive PA) SPSs, the charge conservation governs the whole evolution and annihilation processes.

Up to now, we have established the connections between PA and SPSs with different topological invariants, including ± 1 , ± 2 , and even ± 4 (Table S1 in the Supplemental Material [34]). Then it is logical to think of the possibility of creating other quantized winding numbers of SPSs. One possible way is to consider high-order diffraction channels (i.e., $s_{U_{0,+}} = 1$, $s_{U_{\pm 1,+}} = 0$, $s_{U_{\pm 1,-}}$, $s_{U_{0,-}}$) in Note 5 in the Supplemental Material [34]. But the preassumption of orthogonal modes always leads to $\text{Re}[S_{(U_0, U_{\pm 1})}] > 0$, the ± 1 -order diffraction cannot be desirably eliminated under this situation. Instead, one can consider exciting several nonorthogonal modes by using asymmetric meta-atoms [41]. In analogy with coherent PA [20], it is also possible to consider more than one input channels (i.e., $\tilde{r}_{\pm 1} \neq 0$), which can be expected to find more intriguing phenomena.

In conclusion, we have demonstrated that PA is associated with phase vortices in spectral spaces and reveal its topological behaviors in terms of conserved topological invariants related to SPSs. The intrinsic connection of the evolution of SPSs between radiative and materials losses has been unambiguously established and incorporated with the generation principles of high-order SPSs. Then we reinterpret two basic types of absorbers from the prospects of topology, explaining well the robustness and evolution of absorption spectra as the system parameters change and proposing a strategy to design perfect dual-band absorbers. Our findings connect all the PA phenomena to a wide range of topological defects, vortex physics, phase modulation, etc. We believe that the revealed topological nature in scattering systems and related singular properties will advance the traditional areas of absorbers/emitters and offer opportunities in topological metasurfaces [65] or exception-points-related physics [66].

All associated data and materials are available in the text and Supplemental Material [34].

C.Y.Z. acknowledges the National Natural Science Foundation of China (Grants No. 52120105009 and No. 51906144) and the Shanghai Key Fundamental Research Grant (No. 20JC1414800). C.-W.Q. acknowledges the financial support from the Ministry of Education, Republic of Singapore (Grant No. R-263-000-E19-114) and NRF, Prime Minister's Office, Singapore under the Competitive Research Program Award (Grant No. NRF-CRP26-2021-0063). M.Q.L. acknowledges the support from China Postdoctoral Science Foundation (Grant No. BX20220200) and the SJTU-NUS Joint Ph.D. Project. S.F. acknowledges the support of the U. S. Department of Energy (Grant No. DE-FG02-07ER46426).

M.Q.L. and C.-W.Q. conceived of the ideas. M.Q.L. developed the theory and performed the simulations. M.Q.L., W.J.C., G.W.H., S.F., D.N.C., C.Y.Z., and C.-W.Q. analyzed the data, and all authors discussed the results. M.Q.L. wrote the letter with inputs and comments from all authors. C.Y.Z. and C.-W.Q. supervised the project.

The authors declare no competing interests.

- [1] D. Gevaux, Perfect heat, *Nat. Phys.* **7**, 670 (2011).
- [2] V. S. Asadchy, I. A. Faniayev, Y. Ra'di, S. A. Khakhomov, I. V. Semchenko, and S. A. Tretyakov, Broadband Reflectionless Metasheets: Frequency-Selective Transmission and Perfect Absorption, *Phys. Rev. X* **5**, 031005 (2015).
- [3] I. E. Khodasevych, L. Wang, A. Mitchell, and G. Rosengarten, Micro- and nanostructured surfaces for selective solar absorption, *Adv. Opt. Mater.* **3**, 852 (2015).
- [4] R. Alaei, M. Albooyeh, and C. Rockstuhl, Theory of metasurface based perfect absorbers, *J. Phys. D Appl. Phys.* **50**, 503002 (2017).
- [5] M. Liu and C. Zhao, Ultranarrow and wavelength-scalable thermal emitters driven by high-order antiferromagnetic resonances in dielectric nanogratings, *ACS Appl. Mater. Interfaces* **13**, 25306 (2021).
- [6] D. G. Baranov, Y. Xiao, I. A. Nechepurenko, A. Krasnok, A. Alù, and M. A. Kats, Nanophotonic engineering of far-field thermal emitters, *Nat. Mater.* **18**, 920 (2019).
- [7] B. X. Wang, Y. He, P. Lou, and W. Xing, Design of a dual-band terahertz metamaterial absorber using two identical square patches for sensing application, *Nanoscale Adv.* **2**, 763 (2020).
- [8] D. M. Bierman, A. Lenert, W. R. Chan, B. Bhatia, I. Celanović, M. Soljačić, and E. N. Wang, Enhanced photovoltaic energy conversion using thermally based spectral shaping, *Nat. Energy* **1**, 16068 (2016).
- [9] A. Lenert, D. M. Bierman, Y. Nam, W. R. Chan, I. Celanović, M. Soljačić, and E. N. Wang, A nanophotonic solar thermophotovoltaic device, *Nat. Nanotechnol.* **9**, 126 (2014).
- [10] D. Fan, T. Burger, S. McSherry, B. Lee, A. Lenert, and S. R. Forrest, Near-perfect photon utilization in an air-bridge thermophotovoltaic cell, *Nature (London)* **586**, 237 (2020).
- [11] A. Tittl, A. K. U. Michel, M. Schäferling, X. Yin, B. Gholipour, L. Cui, M. Wuttig, T. Taubner, F. Neubrech, and H. Giessen, A switchable mid-infrared plasmonic perfect absorber with multispectral thermal imaging capability, *Adv. Mater.* **27**, 4597 (2015).
- [12] N. I. Landy, C. M. Bingham, T. Tyler, N. Jokerst, D. R. Smith, and W. J. Padilla, Design, theory, and measurement of a polarization-insensitive absorber for terahertz imaging, *Phys. Rev. B* **79**, 125104 (2009).
- [13] F. Zhang, C. Li, Y. Fan, R. Yang, N.-H. Shen, Q. Fu, W. Zhang, Q. Zhao, J. Zhou, T. Koschny *et al.*, Phase-modulated scattering manipulation for exterior cloaking in metal-dielectric hybrid metamaterials, *Adv. Mater.* **31**, 1903206 (2019).
- [14] A. Berkhout and A. F. Koenderink, Perfect absorption and phase singularities in plasmon antenna array etalons, *ACS Photonics* **6**, 2917 (2019).
- [15] Y. X. Yeng, M. Ghebrehbran, P. Bermel, W. R. Chan, J. D. Joannopoulos, M. Soljačić, and I. Celanovic, Enabling high-temperature nanophotonics for energy applications, *Proc. Nat. Acad. Sci. USA* **109**, 2280 (2012).
- [16] P. Huo, S. Zhang, Y. Liang, Y. Lu, and T. Xu, Hyperbolic metamaterials and metasurfaces: Fundamentals and applications, *Adv. Opt. Mater.* **7**, 1801616 (2019).
- [17] N. Liu, M. Mesch, T. Weiss, M. Hentschel, and H. Giessen, Infrared perfect absorber and its application as plasmonic sensor, *Nano Lett.* **10**, 2342 (2010).
- [18] C. T. Riley, J. S. T. Smalley, J. R. J. Brodie, Y. Fainman, D. J. Sirbully, and Z. Liub, Near-perfect broadband absorption from hyperbolic metamaterial nanoparticles, *Proc. Nat. Acad. Sci. USA* **114**, 1264 (2017).
- [19] C. Y. Yang, J. H. Yang, Z. Y. Yang, Z. X. Zhou, M. G. Sun, V. E. Babicheva, and K. P. Chen, Nonradiating silicon nanoantenna metasurfaces as narrowband absorbers, *ACS Photonics* **5**, 2596 (2018).
- [20] C. Wang, W. R. Sweeney, A. D. Stone, and L. Yang, Coherent perfect absorption at an exceptional point, *Science* **373**, 1261 (2021).
- [21] S. Zanotto, F. P. Mezzapesa, F. Bianco, G. Biasiol, L. Baldacci, M. S. Vitiello, L. Sorba, R. Colombelli, and A. Tredicucci, Perfect energy-feeding into strongly coupled systems and interferometric control of polariton absorption, *Nat. Phys.* **10**, 830 (2014).
- [22] K. V. Sreekanth, S. Han, and R. Singh, Ge₂Sb₂Te₅-Based tunable perfect absorber cavity with phase singularity at visible frequencies, *Adv. Mater.* **30**, 1706696 (2018).
- [23] V. G. Kravets, F. Schedin, R. Jalil, L. Britnell, R. V. Gorbachev, D. Ansell, B. Thackray, K. S. Novoselov, A. K. Geim, A. V. Kabashin *et al.*, Singular phase nano-optics in plasmonic metamaterials for label-free single-molecule detection, *Nat. Mater.* **12**, 304 (2013).
- [24] K. V. Sreekanth, S. Sreejith, S. Han, A. Mishra, X. Chen, H. Sun, C. T. Lim, and R. Singh, Biosensing with the singular phase of an ultrathin metal-dielectric nanophotonic cavity, *Nat. Commun.* **9**, 369 (2018).
- [25] Y. Tsurimaki, J. K. Tong, V. N. Boriskina, A. Semenov, M. I. Ayzatsky, Y. P. Machehkin, G. Chen, and S. V. Boriskina, Topological engineering of interfacial optical tamm states for highly sensitive near-singular-phase optical detection, *ACS Photonics* **5**, 929 (2018).
- [26] Y. Bai, H. Zheng, Q. Zhang, Y. Yu, and S. Liu, Perfect absorption and phase singularities induced by surface lattice resonances for plasmonic nanoparticle array on a metallic film, *Opt. Express* **30**, 45400 (2022).
- [27] Z. Sakotic, A. Krasnok, A. Alù, and N. Jankovic, Topological scattering singularities and embedded eigenstates for polarization control and sensing applications, *Photonics Res.* **9**, 1310 (2021).
- [28] G. Ermolaev, K. Voronin, D. G. Baranov, V. Kravets, G. Tselikov, Y. Stebunov, D. Yakubovsky, S. Novikov, A. Vyshnevyy, A. Mazitov *et al.*, Topological phase singularities in atomically thin high-refractive-index materials, *Nat. Commun.* **13**, 2049 (2022).
- [29] P. A. Thomas, K. S. Menghrajani, and W. L. Barnes, All-optical control of phase singularities using strong light-matter coupling, *Nat. Commun.* **13**, 1809 (2022).
- [30] S. M. Hein and H. Giessen, Retardation-induced phase singularities in coupled plasmonic oscillators, *Phys. Rev. B* **91**, 205402 (2015).
- [31] M. Liu, C. Zhao, Y. Zeng, Y. Chen, C. Zhao, and C.-W. Qiu, Evolution and Nonreciprocity of Loss-Induced Topological Phase Singularity Pairs, *Phys. Rev. Lett.* **127**, 266101 (2021).
- [32] W. Suh and S. Fan, All-pass transmission or flattop reflection filters using a single photonic crystal slab, *Appl. Phys. Lett.* **84**, 4905 (2004).
- [33] W. Suh, Z. Wang, and S. Fan, Temporal coupled-mode theory and the presence of non-orthogonal modes in lossless multimode cavities, *IEEE J. Quantum Electron.* **40**, 1511 (2004).

- [34] See Supplemental Material at <https://link.aps.org/supplemental/10.1103/PhysRevB.107.L241403> for notes: (1) TCMT and generation of SPS; (2) high-order SPS in two-port-two-mode systems; (3) comparison of existing methods for dual-band absorbers; (4) SPS at off-normal incident; (5) possibility of SPS with other orders, which includes Refs. [35–41], Figs. S1–S9, and Table S1.
- [35] J. R. Hendrickson, S. Vangala, C. Dass, R. Gibson, J. Goldsmith, K. Leedy, D. E. Walker, J. W. Cleary, W. Kim, and J. Guo, Coupling of epsilon-near-zero mode to gap plasmon mode for flat-top wideband perfect light absorption, *ACS Photonics* **5**, 776 (2018).
- [36] K. Chen, R. Adato, and H. Altug, Dual-band perfect absorber for multispectral plasmon-enhanced infrared spectroscopy, *ACS Nano* **6**, 7998 (2012).
- [37] B. Zhang, Y. Zhao, Q. Hao, B. Kiraly, I.-C. Khoo, S. Chen, and T. J. Huang, Polarization-independent dual-band infrared perfect absorber based on a metal-dielectric-metal elliptical nanodisk array, *Opt. Express* **19**, 15221 (2011).
- [38] X. Liu, T. Tyler, T. Starr, A. F. Starr, N. M. Jokerst, and W. J. Padilla, Taming the Blackbody with Infrared Metamaterials as Selective Thermal Emitters, *Phys. Rev. Lett.* **107**, 045901 (2011).
- [39] J. Liu, M. Zhu, N. Zhang, H. Zhang, Y. Zhou, S. Sun, N. Yi, S. Gao, Q. Song, and S. Xiao, Wafer-scale metamaterials for polarization-insensitive and dual-band perfect absorption, *Nanoscale* **7**, 18914 (2015).
- [40] Y. H. Kan, C. Y. Zhao, X. Fang, and B. X. Wang, Designing ultrabroadband absorbers based on Bloch theorem and optical topological transition, *Opt. Lett.* **42**, 1879 (2017).
- [41] Z. Fan, M. R. Shcherbakov, M. Allen, J. Allen, B. Wenner, and G. Shvets, Perfect diffraction with multiresonant bianisotropic gratings, *ACS Photonics* **5**, 4303 (2018).
- [42] B. X. Wang, M. Q. Liu, T. C. Huang, and C. Y. Zhao, Micro/nanostructures for far-field thermal emission control: An overview, *ES Energy Environ.* **6**, 18 (2019).
- [43] W. Li and S. Fan, Nanophotonic control of thermal radiation for energy applications [Invited], *Opt. Express* **26**, 15995 (2018).
- [44] J. Wang, A. Chen, Y. Zhang, J. Zeng, Y. Zhang, X. Liu, L. Shi, and J. Zi, Manipulating bandwidth of light absorption at critical coupling: An example of graphene integrated with dielectric photonic structure, *Phys. Rev. B* **100**, 075407 (2019).
- [45] C. Qu, S. Ma, J. Hao, M. Qiu, X. Li, S. Xiao, Z. Miao, N. Dai, Q. He, S. Sun *et al.*, Tailor the Functionalities of Metasurfaces Based on a Complete Phase Diagram, *Phys. Rev. Lett.* **115**, 235503 (2015).
- [46] W. Chen, Q. Yang, Y. Chen, and W. Liu, Evolution and global charge conservation for polarization singularities emerging from non-hermitian degeneracies, *Proc. Nat. Acad. Sci. USA* **118**, e2019578118 (2021).
- [47] B. Zhen, C. W. Hsu, L. Lu, A. D. Stone, and M. Soljačić, Topological Nature of Optical Bound States in the Continuum, *Phys. Rev. Lett.* **113**, 257401 (2014).
- [48] Y. Guo, M. Xiao, and S. Fan, Topologically Protected Complete Polarization Conversion, *Phys. Rev. Lett.* **119**, 167401 (2017).
- [49] N. D. Mermin, The topological theory of defects in ordered media, *Rev. Mod. Phys.* **51**, 591 (1979).
- [50] M. Zürch, C. Kern, P. Hansinger, A. Dreischuh, and C. Spielmann, Strong-field physics with singular light beams, *Nat. Phys.* **8**, 743 (2012).
- [51] L. Du, A. Yang, A. V. Zayats, and X. Yuan, Deep-subwavelength features of photonic skyrmions in a confined electromagnetic field with orbital angular momentum, *Nat. Phys.* **15**, 650 (2019).
- [52] Y. Wang, Z.-L. Deng, D. Hu, J. Yuan, Q. Ou, F. Qin, Y. Zhang, X. Ouyang, Y. Li, B. Peng *et al.*, Atomically thin noble metal dichalcogenides for phase-regulated meta-optics, *Nano Lett.* **20**, 7811 (2020).
- [53] M. Kang, S. Zhang, M. Xiao, and H. Xu, Merging Bound States in the Continuum at off-High Symmetry Points, *Phys. Rev. Lett.* **126**, 117402 (2021).
- [54] J. R. Piper, V. Liu, and S. Fan, Total absorption by degenerate critical coupling, *Appl. Phys. Lett.* **104**, 251110 (2014).
- [55] A. Cattoni, P. Ghenuche, A.-M. Haghiri-Gosnet, D. Decanini, J. Chen, J.-L. Pelouard, and S. Collin, $\lambda^3/1000$ plasmonic nanocavities for biosensing fabricated by soft UV nanoimprint lithography, *Nano Lett.* **11**, 3557 (2011).
- [56] Y. Xiang, L. Wang, Q. Lin, S. Xia, M. Qin, and X. Zhai, Tunable dual-band perfect absorber based on L-shaped graphene resonator, *IEEE Photonics Technol. Lett.* **31**, 483 (2019).
- [57] S. Liu, H. Chen, and T. J. Cui, A broadband terahertz absorber using multi-layer stacked bars, *Appl. Phys. Lett.* **106**, 151601 (2015).
- [58] X. Ming, X. Liu, L. Sun, and W. J. Padilla, Degenerate critical coupling in all-dielectric metasurface absorbers, *Opt. Express* **25**, 24658 (2017).
- [59] H. Li, G. Wei, H. Zhou, H. Xiao, M. Qin, S. Xia, and F. Wu, Polarization-independent near-infrared superabsorption in transition metal dichalcogenide Huygens metasurfaces by degenerate critical coupling, *Phys. Rev. B* **105**, 165305 (2022).
- [60] R. Xu and J. Takahara, Radiative loss control of an embedded silicon perfect absorber in the visible region, *Opt. Lett.* **46**, 805 (2021).
- [61] J. Yu, B. Ma, A. Ouyang, P. Ghosh, H. Luo, A. Pattanayak, S. Kaur, M. Qiu, P. Belov, and Q. Li, Dielectric super-absorbing metasurfaces via PT symmetry breaking, *Optica* **8**, 1290 (2021).
- [62] M. S. Sidorenko, O. N. Sergaeva, Z. F. Sadrieva, C. Roques-Carnes, P. S. Muraev, D. N. Maksimov, and A. A. Bogdanov, Observation of an Accidental Bound State in the Continuum in a Chain of Dielectric Disks, *Phys. Rev. Appl.* **15**, 034041 (2021).
- [63] X. Zhao, C. Chen, K. Kaj, I. Hammock, Y. Huang, R. D. Averitt, and X. Zhang, Terahertz investigation of bound states in the continuum of metallic metasurfaces, *Optica* **7**, 1548 (2020).
- [64] T. Yoda and M. Notomi, Generation and Annihilation of Topologically Protected Bound States in the Continuum and Circularly Polarized States by Symmetry Breaking, *Phys. Rev. Lett.* **125**, 053902 (2020).
- [65] C. W. Qiu, T. Zhang, G. Hu, and Y. Kivshar, Quo vadis, metasurfaces? *Nano Lett.* **21**, 5461 (2021).
- [66] Q. Song, M. Odeh, J. Zúñiga-Pérez, B. Kanté, and P. Genevet, Plasmonic topological metasurface by encircling an exceptional point, *Science* **373**, 1133 (2021).